Density Functional Theory Study of Degradation of Tetraalkylammonium Hydroxides

ARTICLE *in* THE JOURNAL OF PHYSICAL CHEMISTRY C · JUNE 2010

Impact Factor: 4.77 · DOI: 10.1021/jp9122198

Density Functional Theory Study of Degradation of Tetraalkylammonium Hydroxides

Shaji Chempath,[†] James M. Boncella,[§] Lawrence R. Pratt,[||] Neil Henson,[†] and Bryan S. Pivovar*[,‡]

Theoretical Division, Los Alamos National Laboratory, Los Alamos, New Mexico 87545, National Renewable Energy Laboratory, Golden, Colorado 80401, Materials Physics and Applications, Los Alamos National Laboratory, Los Alamos, New Mexico 87545, and Department of Chemical and Biomolecular Engineering, Tulane University, New Orleans, Louisiana 70118

Received: December 28, 2009; Revised Manuscript Received: May 12, 2010

We report density functional theory (DFT) studies of the degradation mechanism of tetraalkylammonium cations which are of interest for anion exchange membrane fuel cells. Three mechanisms of attack by hydroxide anions are explored: an S_N2 pathway leading to alcohol formation, an ylide pathway that gives rise to unstable intermediates, and Hofmann elimination. Tetramethylammonium, ethyltrimethylammonium, and benzyltrimethylammonium are the model cations studied here. S_N2 attack on tetramethylammonium was found to have a free energy barrier of 17.0 kcal/mol at 298 K. In the case of ethyltrimethylammonium, the overall barrier for the S_N2 pathway was found to be 23.0 kcal/mol while Hofmann elimination was 12.8 kcal/mol. The ylide and S_N2 attacks on benzyltrimethylammonium show similar energy changes as in the case of tetramethylammonium. In the case of benzyltrimethylammonium, additional side reactions starting from the ylide intermediate are also shown to be feasible. We also discuss the influence of the immediate solvation shell on the reaction mechanism. A refined model in which the immediate solvation shell of hydroxide is modeled explicitly is found to have better experimental agreement than a model in which solvation is modeled implicitly.

Introduction

Tetraalkylammonium cations (e.g., $N(CH_3)_4^+$) are known to degrade under aqueous conditions at high pH, primarily due to attack by the hydroxide counterion.[1−5] Among the many applications of tetraalkylammonium ions, their possible use in alkaline anion exchange membranes (AAEM) has received recent attention.[6,7] These cations can be tethered to a polymer backbone and the resulting material can be used as the polymer electrolyte membrane (PEM) in an alkaline membrane fuel cell (AMFC).[8,9] However, the tendency of these cations to react with aqueous hydroxide (OH^-) under fuel cell operating conditions is one of the limitations that is preventing AMFCs from being widely used. Target AMFC operating conditions may be 60−100 °C, where membranes may contain 10−50 absorbed water molecules per cation. If AMFCs can be successfully demonstrated they will likely displace current polymeric, acid based fuel cells in many applications. Acidic membrane fuel cells use precious metals such as Pt or Ru as the catalyst in their electrodes, whereas AMFCs allow for the use of nonprecious metal catalysis.[10] Recently, Lu et al.[9] demonstrated an alkaline fuel cell that did not use any noble metal catalysis. The membrane in their fuel cell used quarternary ammonium polysulfone and was demonstrated at only 60 °C, presumably because the quarternary ammonium group is not stable at higher temperatures. There is clearly a need for identifying cations that are chemically stable in the temperature range of 60−100 °C in aqueous alkaline conditions.

In our previous work,[6] we reported computational studies on the stability of tetramethylammonium ($[N(CH_3)_4^+]$) under aqueous conditions in the presence of OH^- ion. Two reaction paths, both of which lead to the same final reaction products, were identified. In the S_N2 pathway, nucleophilic attack by OH^- on the CH_3 group produces trimethylamine and methanol. In the other pathway denoted as the ylide pathway, OH^- abstracts a proton from a CH_3 group and produces a water molecule along with an ylide intermediate ($N(CH_3)_3^+-CH_2^-$). This intermediate in turn reacts to give the final products, trimethylamine and methanol. By changing the dielectric constant of the medium used in our DFT calculations, we also found that the rate of degradation increases with decreasing water content in the reaction medium. Experimental results on the thermogravimetry (TG) and mass spectroscopy (MS) of $N(CH_3)_4OH\cdot 5H_2O$ were also reported.[6,11] An exchange between the aqueous and methyl hydrogens (as observed with deuterated water) confirmed our prediction of an ylide pathway. Almost all the previous work on AAEMs suggests that anion exchange membranes are not stable for extended periods of time in the hydroxide form at temperatures above 60 °C. Hatch and Lloyd[1] and Baumann[2] studied the stability of membranes made from polymers with benzyltrimethylammonium side chains and concluded that S_N2 attack on benzyl and methyl groups is the main reason for membrane instability above 60 °C. The Hofmann elimination reaction, which involves hydroxide attack on aliphatic hydrogens at the β-position relative to the quarternary nitrogen, has also been reported as another mechanism of degradation of tetraalkylammonium ions.[12−14] Tomoi et al.[14] modified the linker between the benzene ring and the quarternary nitrogen in anion exchange resins and found improved performance with linkers such as

* To whom correspondence should be addressed: 1617 Cole Blvd, Golden, CO, 80401. Fax: 303-275-2840. Phone: 303-275-3809. E-mail: bryan_pivovar@nrel.gov.
[†] Theoretical Division, Los Alamos National Laboratory.
[§] Materials Physics and Applications, Los Alamos National Laboratory.
[||] Tulane University.
[‡] National Renewable Energy Laboratory.

10.1021/jp9122198
Published on Web 06/22/2010

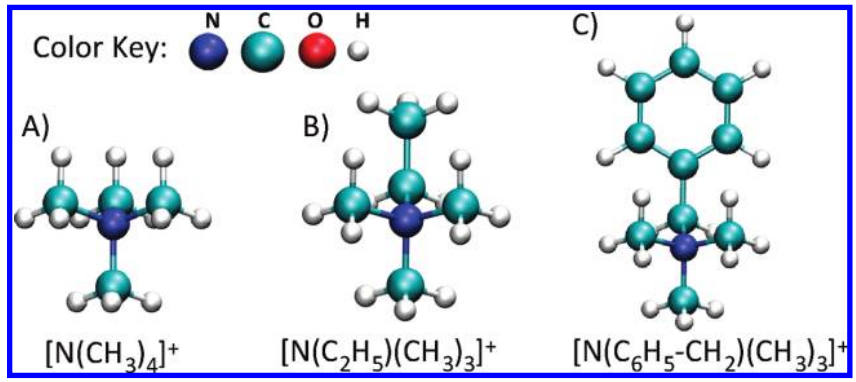

Figure 1. The three cations studied in this paper: (A) tetramethylammonium (TMA), (B) ethyltrimethylammonium (ethyl-TMA), and (C) benzyltrimethylammonium (benzyl-TMA). The color key used in all figures is also shown.

hexyleneoxymethylene. Other studies in the literature have concentrated on the detailed mechanism of degradation of benzyltrimethylammonium, especially from the point of view of ylide rearrangements. Ylide intermediates formed by OH^- attack on benzyltrimethylammonium can undergo further degradation through the Stevens rearrangement or Sommelet−Hauser mechanisms.[4,15−17] Ab initio electronic structure studies were used by Heard and Yates to conclude that Stevens and Sommelet−Hauser rearrangements had similar activation energy barriers.[18−20]

In this paper we concentrate on the degradation of the three alkylammonium cations shown in Figure 1, namely tetramethylammonium $N(CH_3)_4^+$, ethyltrimethylammonium $N(CH_3)_3(C_2H_5)^+$, and benzyltrimethylammonium $N(CH_3)_3(C_6H_5CH_2)^+$. These cations will be referred to as TMA, ethyl-TMA, and benzyl-TMA, respectively. From a practical point of view, the ethyl and benzyl versions are more relevant because a benzyl group or an aliphatic chain will be used to link the quarternary nitrogen to a polymer backbone (our earlier studies showed a phenyl linked version had much lower stability than the benzyl version[11]). Ethyl-TMA, which has β-hydrogens, also serves as a model cation for studying Hofmann elimination reactions. In the case of our simplest cation, TMA, we also look at further corrections to our computational model, aimed at understanding the effect of an immediate solvation shell. A comparison between experiment and theory is achieved by comparing the activation barriers obtained from theory against those estimated from experimental data.

Methods

Energies and structures of all the cations studied in this paper are obtained with B3LYP density functional theory using the 6-311++g(2d,p) basis set as implemented in Gaussian 03 (G03) software.[21] We report energy changes (ΔE) and standard free energy changes (ΔG^0) for all the reactions. For a model reaction A + B → C, we optimize the geometries of species A, B, and C in a dielectric medium of $\varepsilon = 80$ (corresponding to water). The Polarizable Continuum Model (PCM) in G03 is used to evaluate the effect of the medium on the solute electronic structure and to estimate the interaction energy between the solute and the dielectric medium. The self-consistent field (SCF) energy reported by G03 includes the electronic energy of the solute and the interactions with the dielectric medium. The difference in SCF energies gives $\Delta E = E_{SCF}(C) - (E_{SCF}(A) + E_{SCF}(B))$. Vibrational frequency calculations of the optimized structures are performed to calculate the standard free energies of all chemical species involved in the reaction and also the standard free energy change for the process, $\Delta G^0 = G^0(C) - (G^0(A) + G^0(B))$.

The standard free energy of a chemical species is calculated by adding the following terms to E_{SCF}: cavity formation energy, van der Waals interactions, translational free energy, quantum mechanical rotational and vibrational free energies, and zero point energy, all as reported by G03 software. For estimating activation barriers, we conducted reaction path studies with a growing string method.[22] For the model reaction A + B → C, we optimize a reaction complex [AB], which contains both the reactants placed adjacent to each other and optimized in the dielectric medium. The growing string method finds intermediate structures on the minimum energy path (MEP) connecting the reactant [AB] to the product C. The highest energy structure on the MEP is taken as the first approximation for a transition state. The exact transition state $[AB]^‡$ (the saddle point on the potential energy surface) is obtained from this approximate point by using the Berny optimization algorithm as implemented in G03. Then the activation energy and free energy barriers for that reaction are defined as $\Delta E^‡ = E_{SCF}([AB]^‡) - (E_{SCF}(A) + E_{SCF}(B))$, and $\Delta G^{‡,0} = G^0([AB]^‡) - (G^0(A) + G^0(B))$. We use a concentration of 1 mol/L as the standard state and the free energies are reported at 298 K unless otherwise mentioned. At 298 K we added 1.9 kcal/mol to the free energies reported by G03, to convert the standard state from 1/22.4 mol/L to 1 mol/L. In some cases the frequency analysis and free energy evaluations were repeated at temperatures other than 298 K to make comparisons against available experimental data. Initial geometry optimizations and frequency analyses were carried out with a 6-31G(d) basis set with the PCM model, followed by a further geometry optimization with a 6-311+G(2d,p) basis set also with the PCM model, but omitting the frequency calculation. Thus the vibrational free energy contributions are evaluated at b3lyp/6-31 g(d) level theory.

Results and Discussion

Degradation of Tetramethylammonium. In our previous letter[6] we discussed the degradation mechanism of TMA through two pathways: an S_N2 path way and an ylide pathway.

The S_N2 reaction,

$$[N(CH_3)_4]^+ + OH^- \rightarrow N(CH_3)_3 + CH_3OH \qquad (1)$$

is thermodynamically downhill ($\Delta E = -25.3$ kcal/mol, $\Delta G^0 = -28.7$ kcal/mol), and the activation barrier of the reaction was found to be $\Delta G^{‡,0} = 17.0$ kcal/mol. The ylide pathway consists of the following two steps:

$$[N(CH_3)_4]^+ + OH^- \rightarrow (CH_2)^- - N^+(CH_3)_3 + H_2O \quad (2a)$$

$$(CH_2)^- - N^+(CH_3)_3 + H_2O \rightarrow N(CH_3)_3 + CH_3OH \quad (2b)$$

In the first step of the ylide pathway, the OH^- abstracts a proton from one of the methyl groups to form trimethylammonium methylide ($N(CH_3)_3^+-CH_2^-$) and a water molecule ($\Delta G^{\ddagger,0} = 9.2$ kcal/mol). In the second step the ylide reacts with water to form $N(CH_3)_3$ and CH_3OH. Structures of the intermediates and energy changes along the reaction paths are shown in Figure 2. The transition state for the second step (reaction 2b) is exactly the same as the one for the S_N2 pathway. Thus the rate of degradation calculated through both pathways is exactly the same. However the identification of the ylide pathway has many important consequences. First of all, it explains the H−D exchange observed in the TG-MS experiments conducted with $[N(CH_3)_4^+][OD^-]\cdot 5D_2O$.[23] The exchange between methyl H atoms and aqueous D atoms is possible only with the ylide pathway. The S_N2 pathway does not allow for any scrambling between methyl and aqueous hydrogen/deuterium atoms. Second, the ylide intermediate may lead to additional side reactions which were not anticipated before (inter- or intramolecular reactions including rearrangement reactions). For example, the ylide intermediate could react with the linker or the backbone of the polymer, when the cation is used in an anion-exchange membrane. Third, the ylide pathway may also become the prevalent pathway under dry conditions,[5,24] since water is one of the products released in reaction 2a.

An important point to note is that the minimum corresponding to the ylide (point F in the ylide path in Figure 2) is very shallow, which implies that the ylide is unstable. A further discussion of ylide formation is given at the end of this paper.

Degradation of Benzyltrimethylammonium. Benzyl-TMA, which has two types of carbon atoms (methyl and benzyl) amenable to attack by OH^-, can degrade along two S_N2 pathways and two ylide pathways. These reactions and the energy changes are listed in Table 1. It can be seen that the activation free energy barriers for S_N2 attack on the methyl and benzyl carbons are very similar to each other (18.9 and 18.6 kcal/mol) and to the barrier for S_N2 attack on $N(CH_3)_4^+$ (17.0 kcal/mol). This implies that the intrinsic stabilities of the benzyl cations are very close to that of $N(CH_3)_4^+$. However, we point out that the C−O distance for the transition state during the

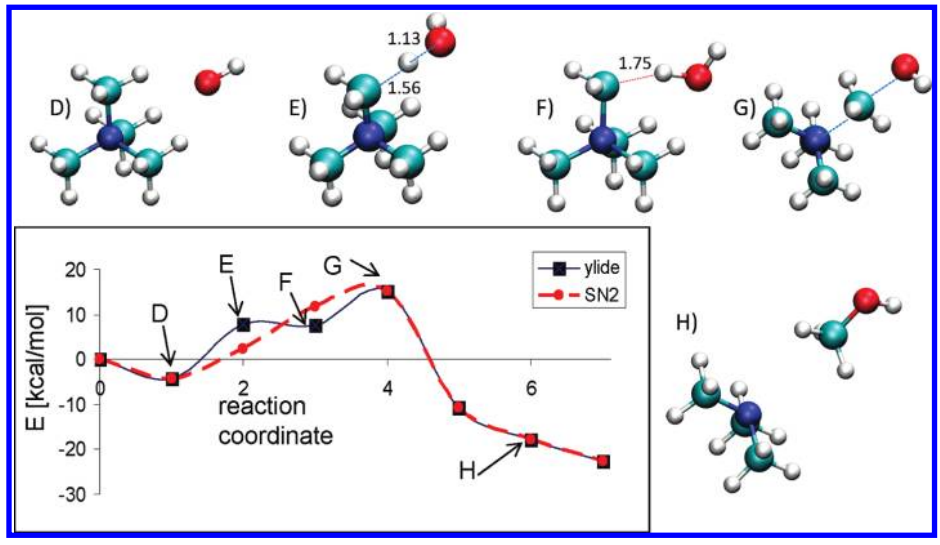

Figure 2. Minimum energy paths and geometries along S_N2 and ylide pathways. The letters D to H are used to denote the structures and identify them on the minimum energy paths shown above. All geometries were optimized with the PCM model and B3LYP/6-311++G(2d,p) level theory: (D) the reactant complex: TMA^+ and OH^-; (E) transition state for ylide formation; (F) ylide−water complex; (G) the common transition state for reactions 1 and 2b; and (H) the product complex: trimethylamine and methanol. Distances between selected atoms are given in Å.

TABLE 1: Energy Changes (in kcal/mol) for Reactions of Benzyl-TMA[a]

eq no.	equation	ΔE	ΔG^0	$\Delta E^{\ddagger}$	$\Delta G^{\ddagger,0}$
3	$N(CH_3)_3(CH_2-C_6H_5) + OH^- \rightarrow N(CH_3)_3+C_6H_5-CH_2OH$ (3)	−29.5	−32.9	13.9	18.9
4	$N(CH_3)_3(CH_2-C_6H_5) + OH^- \rightarrow N(CH_3)_2(C_6H_5-CH_2) + CH_3OH$ (4)	−25.3	−27.4	15.3	18.6
5	$N(CH_3)_3(CH_2-C_6H_5) + OH^- \rightarrow (CH_3)_3N^+-(C_6H_5-CH)^- + H_2O$ (5)	7.260	14.5	7.337	11.1
6	$N(CH_3)_3(CH_2-C_6H_5) + OH^- \rightarrow (CH_3)_2(C_6H_5-CH_2)N^+-(CH_2)^- + H_2O$ (6)	8.357	13.2	8.365	10.9

[a] Reactions 3 and 4 correspond to S_N2 attack and reactions 5 and 6 correspond to ylide formation. For reactions 5 and 6 the energy changes correspond to the case where the water molecule is still attached to the ylide.

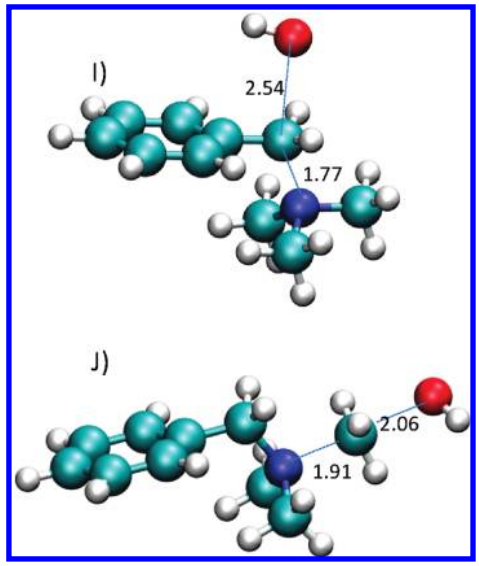

Figure 3. Transition state structures for S_N2 attack on benzyl (I) and methyl (J) carbons of benzyl-TMA. Even though the energies for these structures are almost equal, the C−O distance is larger by 0.48 Å in structure I (see text).

S_N2 attack on benzyl carbon (2.54 Å) is larger compared to the C−O distance for the attack on the methyl carbon (2.06 Å) as shown in Figure 3. In the case of ylide formation, again, the activation energies barriers for attack on benzyl and methyl hydrogens are very similar (reactions 5 and 6 in Table 1). Also, these energy barriers are close to the barrier for attack on the methyl hydrogens of $[N(CH_3)_4^+]$ through reaction 2a. It should be pointed out that the transition state and final product are very close in energy for some reactions ($\Delta E = 7.260$ kcal/mol, $\Delta E^{\ddagger} = 7.337$ kcal/mol). This shows that the energy profile is essentially flat between the transition state structure and the product structure.

Degradation of Ethyltrimethylammonium. In the presence of hydrogen atoms in the position β to the nitrogen atom, Hofmann elimination reactions become feasible. OH^- attack on the ethyl group leads to the formation of ethylene and water as shown:

$$N(CH_3)_3(C_2H_5)^+ + OH^- \rightarrow N(CH_3)_3 + C_2H_4 + H_2O \quad (7)$$

The reactants, products, and transition states for this reaction are shown in Figure 4. The calculated barrier $\Delta G^{\ddagger,0}$ for this reaction is only 12.8 kcal/mol, indicating that the Hofmann elimination is more probable compared to the S_N2 attack. S_N2 attack on the ethyl carbon leads to the formation of ethanol with a barrier of 23.2 kcal/mol, whereas the S_N2 attack on the CH_3 group leads to methanol formation has a barrier of 19.4 kcal/mol. The presence of the ethyl group seems to prevent the formation of a stable ylide. We were not able to minimize a geometry corresponding to the ylide $N(CH_3)_2(C_2H_5)^+-CH_2^-(H_2O)$, which appears on the right-hand side of reaction 10 in Table 2.

Effect of Using a Refined Model with Explicit Water Molecules. In the computational model used here, we have not explicitly accounted for the chemical interactions between the hydroxide species and the water molecules in its immediate neighborhood. The PCM model approximately accounts for the effect of dielectric constant that is surrounding the reaction center. However, it does not take into account the specific OH^-−water chemical interactions. One way to refine our predictions is to explicitly include water molecules around the OH^- to reflect its natural solvation shell in an aqueous environment.

We take the solvated OH^- with three water molecules as one of the reactants, with the cation being the other reactant. One could add more water molecules around the reactants and expect to create a better model. However, such calculations will need to take into account the various orientations that can be adopted by the water molecules and there will be numerous degrees of freedom to consider. Also, the free energy calculations and energy minimizations in the presence of the PCM become increasingly cumbersome and difficult to converge. The reaction in the explicit model can be written as

$$N(CH_3)_{4(aq)}^+ + OH^-(H_2O)_{3(aq)} \rightarrow N(CH_3)_4OH(H_2O)_{3(aq)} \quad (11a)$$

$$N(CH_3)_4OH(H_2O)_{3(aq)} \rightarrow N(CH_3)_{3(aq)} + CH_3OH(H_2O)_{3(aq)} \quad (11b)$$

We would like to point out that eq 11a does not imply OH^- remain tetrahedrally coordinated to three water molecules in an aqueous environment. We have chosen $OH^-(H_2O)_3$ as a small and simple model for solvated OH^- ion. There have been many studies in the literature aimed at understanding the solvation of OH^-, especially trying to understand if it is 3-coordinated (tetrahedral $OH^-(H_2O)_3$) or 4-coordinated (hypercoordinated or square planar $OH^-(H_2O)_4$).[25−33] An exhaustive review of this subject can be found in Tuckerman et al,[31] where arguments are given to prove that OH^-(aq) is mostly hypercoordinated. The implications of such a possibility (OH^- being 4-coordinated) will be discussed below.

The reactants, activation states, and products are shown in Figure 5. In reactions 11a and 11b we have used the subscript (aq) to emphasize that all the species are surrounded by a PCM water model with a dielectric constant of 80. The energy changes

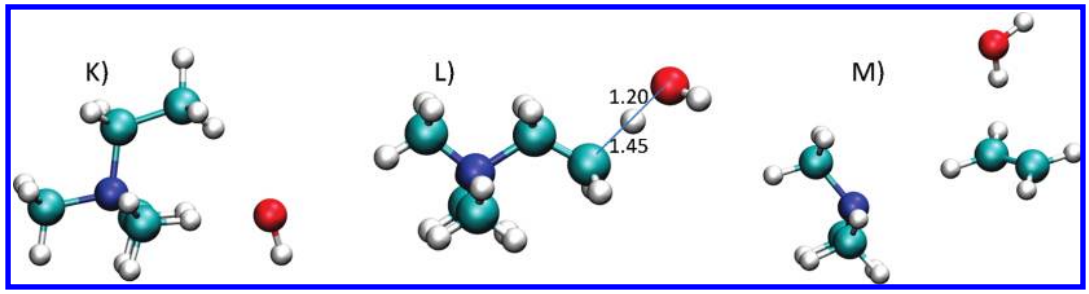

Figure 4. Hofmann elimination on ethyl-TMA leading to the release of ethylene and water: (K) optimized geometry of the reactant complex ethyl-TMA and OH^-; (L) transition state for Hofmann elimination; and (M) product complex: trimethylamine, ethylene, and water.

TABLE 2: Energy Changes (in kcal/mol) for Reactions of Ethyl-TMA[a]

eq no.	equation	ΔE	ΔG^0	$\Delta E^{\ddagger}$	$\Delta G^{\ddagger,0}$
8	$[N(CH_3)_3(C_2H_5)]^+ + OH^- \rightarrow N(CH_3)_3 + C_2H_5OH$ (8)	−28.7	−30.7	18.8	23.2
9	$N(CH_3)_3(C_2H_5) + OH^- \rightarrow N(CH_3)_2(C_2H_5) + CH_3OH$ (9)	−24.1	−26.2	15.7	19.4
7	$N(CH_3)_3(C_2H_5) + OH^- \rightarrow N(CH_3)_3 + C_2H_4 + H_2O$ (7a)	−18.5	−30.8	12.0	12.8
10	$N(CH_3)_3(C_2H_5) + OH^- \rightarrow (CH_3)_2(C_2H_5)N^+-(CH_2)^-(H_2O)$ (10)	not feasible			

[a] Reactions 8 and 9 correspond to S_N2 attack, reaction 7 is the Hofmann elimination, and reaction 10 is not feasible because the geometry of the product ($(CH_3)_2(C_2H_5)N^+-(CH_2)^-(H_2O)$, an ylide with a water molecule) does not correspond to an energy minimum.

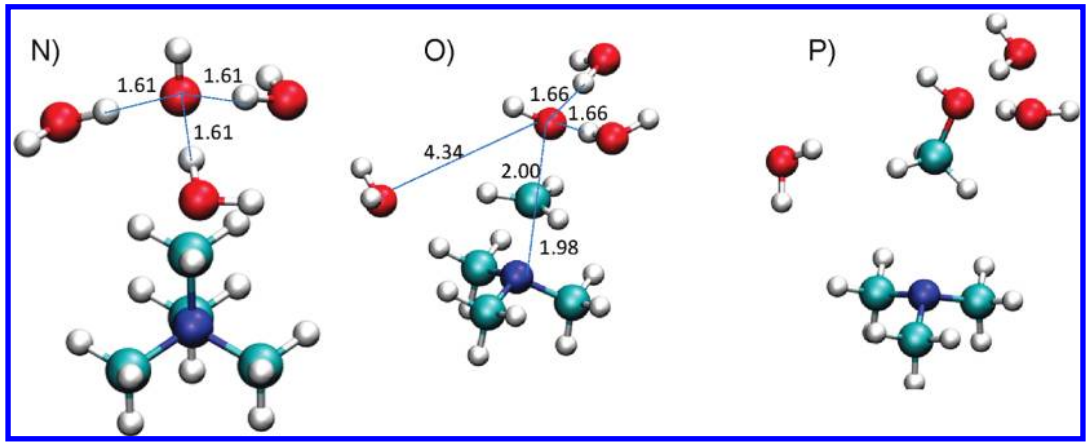

Figure 5. S_N2 attack on trimethylammonium with three solvent molecules modeled explicitly and the rest of the solvent medium implicitly with PCM: (N) reactant complex with TMA^+ and $OH^-\cdot(H_2O)_3$; (O) in the transition state one of the water molecules is pushed away to a distance of 4.34 Å from the OH^-; and (P) the product complex: trimethylamine, methanol and 3 water molecules.

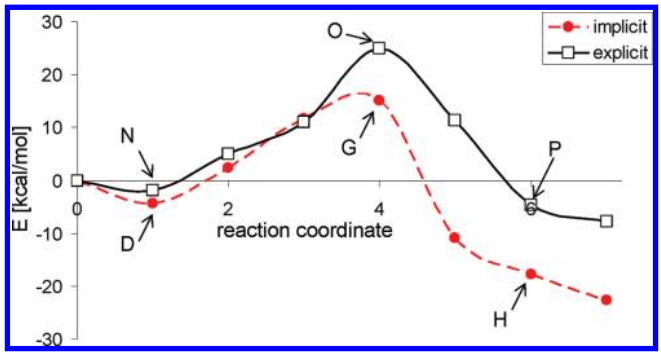

Figure 6. Energy change along the minimum energy path for S_N2 attack by OH^- on TMA with implicit and explicit models. The letters N, O, and P refers to the structures in Figure 5, and the letters D, G, and H refers to the structures in Figure 2.

and activation barrier are remarkably different from the revised model. The $\Delta G^{\ddagger,0}$ has increased to 29.3 kcal/mol, which is higher by 12.3 kcal/mol compared to the value from the previous model. Energy changes along the minimum energy path for the explicit model are shown in Figure 6. A visualization of the structural changes along the reaction path revealed that one of the three water molecules surrounding the OH^- loses its hydrogen bond prior to the umbrella inversion of the CH_3 group. After losing one of the water molecules, the OH^- positions itself so that the C−O−H angle is around 104° and then proceeds with S_N2 attack. This can be seen in the transition state shown in Figure 5, where one of the water molecules is situated 4.34 Å away from the OH^-. The change in $\Delta G^{\ddagger,0}$ by +12.3 kcal/mol can be considered as a correction to the $\Delta G^{\ddagger,0}$ values for S_N2 attack obtained with the implicit model. Note that we have used a 3-coordinated OH^- ion here. If we had used a 4-coordinated OH^- as the reactant, the overall free energy changes would have been amended by the free energy required to first shed the fourth water molecule. It is reasonable to presume that this shedding of an additional water molecule would increase the overall free energy barrier, likely by a few kilocalories per mole.

Comparison of $\Delta G^{\ddagger,0}$ from Theory and Experiment. An estimate of the rate can be obtained with the application of transition state theory, where the rate constant in the absence of tunneling effects is given by $k_{TST} = (k_B T/h) \exp(-\Delta G^{\ddagger,0}/RT)$. In the case of bimolecular reactions, the rate constant k_{TST} can be applied assuming that the free energies are calculated with respect to a standard state (1 mol/L in this paper) and concentrations are expressed in units of the standard state. Also, given an experimentally observed rate, one could estimate an apparent activation barrier $\Delta G^{\ddagger,0}$. In the previous subsection we identified a correction of +12.3 kcal/mol for the S_N2 barrier obtained for tetramethylammonium with the implicit model. Unfortunately, we do not have any experimentally observed rate constants for TMA. However, we could apply the correction of +12.3 kcal/mol to the calculated $\Delta G^{\ddagger,0}$ for benzyl-TMA and make comparisons against values observed in experiments. The observed rate constant at 120 °C for benzyl-TMA is 3.2×10^{-3} L/mol/s, which corresponds to $\Delta G^{\ddagger,0} = 28.8$ kcal/mol at 120 °C. Our theoretical prediction for S_N2 attack on the benzyl group with implicit model was 18.9 kcal/mol at 298 K, which after

TABLE 3: Activation Energy Barrier $\Delta E^{\ddagger}$ for S_N2 Attack on TMA with Implicit Model

theory	B3LYP		MP2		
basis set	6-31+g(d,p)	6-311++g(2d,p)	6-311++g(2d,p)	aug-cc-pvdz	aug-cc-pvdz
kcal/mol	13.4	13.05	16.18	15.82	16.27

the correction becomes 31.1 kcal/mol. Thus, the explicit modeling of the immediate solvation shell brings the experimental and theory $\Delta G^{\ddagger,0}$ values closer to each other. However, we have to take into account the change in temperature. After re-evaluating the thermodynamics at 120 °C and applying the correction we obtain a value of $\Delta G^{\ddagger,0} = 34.0$ kcal/mol, slightly higher than the value 28.8 kcal/mol obtained from experiment. To check the validity of our correction procedure, we also evaluated the $\Delta G^{\ddagger,0}$ for S_N2 attack on benzyl-TMA by reoptimizing the transition state with three added water molecules. We were not able to obtain the entire minimum energy path due to the computational difficulties involved with this larger system. The $\Delta G^{\ddagger,0}$ obtained for this explicit model for benzyl-TMA is 35.3 kcal/mol at 120 °C, which is close to the 34.0 kcal/mol obtained from the implicit model with the correction applied. These findings confirm that accounting for the immediate neighborhood of OH^- by the addition of explicit water molecules is very important to be able to understand the degradation of these cations. In the absence of such corrections we would have predicted the rate of degradation rate constant for benzyl-TMA at 80 °C to be 12.7 L/mol/s, whereas our experiments show that benzyl degradation rates are much lower (only 10% degradation in 700 h at 80 °C, which correspond to 4×10^{-3} L/mol/s). It should be noted that tunneling effects have lower importance for the reactions that involve the S_N2 transition state, because the heavier oxygen and carbon atoms are part of the reaction center. However, tunneling corrections to TST will be important for the proton transfer reactions involving lighter hydrogen atoms discussed in context of ylide formations below.

We also checked the accuracy of our electronic structure calculations by re-evaluating $\Delta E^{\ddagger}$ for S_N2 attack on TMA with MP2 theory and different basis sets. The geometries were optimized at different levels of theory and energies were recalculated. The results in Table 3 show that different levels of theory lead to energies in the range of 13.05 to 16.27 kcal/mol, a spread of 1.61 kcal/mol.

Why Is Ylide Important? Our identification of the ylide pathway[6] clearly explained the observed exchange of hydrogen/deuterium atoms between the cations and the aqueous medium through the following steps:

$$N(CH_3)_4^+ + OD^- \rightarrow N(CH_3)_3^+ - CH_2^-(HOD) \quad (12a)$$

$$N(CH_3)_3^+ - CH_2^-(HOD) + D_2O \rightarrow N(CH_3)_3^+ - CH_2^-(D_2O) + HOD \quad (12b)$$

$$N(CH_3)_3^+ - CH_2^-(D_2O) \rightarrow N(CH_3)_3(CH_2D)^+ + OD^- \quad (12c)$$

Previously we had not shown that the middle step (reaction 12b) had small energy barriers. Reaction 12b consists of the displacement of a water molecule that is tightly bound to the ylide and the arrival of another water molecule in its place. We investigated this reaction path and estimated the activation barrier for this process to be around 21 kcal/mol. This relatively low barrier corresponds to an exchange rate of 0.4 L/mol/s at 80 °C. The addition of tunneling corrections to proton transfer reactions involving ylides will make these rates even higher relative to the rates without tunneling corrections. While we do not have any rate of exchange measurements, TG-MS experiments suggest rapid scrambling of aqueous and methyl hydrogens.[23] The relatively low activation barrier estimated from minimum energy path calculations is consistent with this exchange proceeding through the formation of an ylide intermediate.

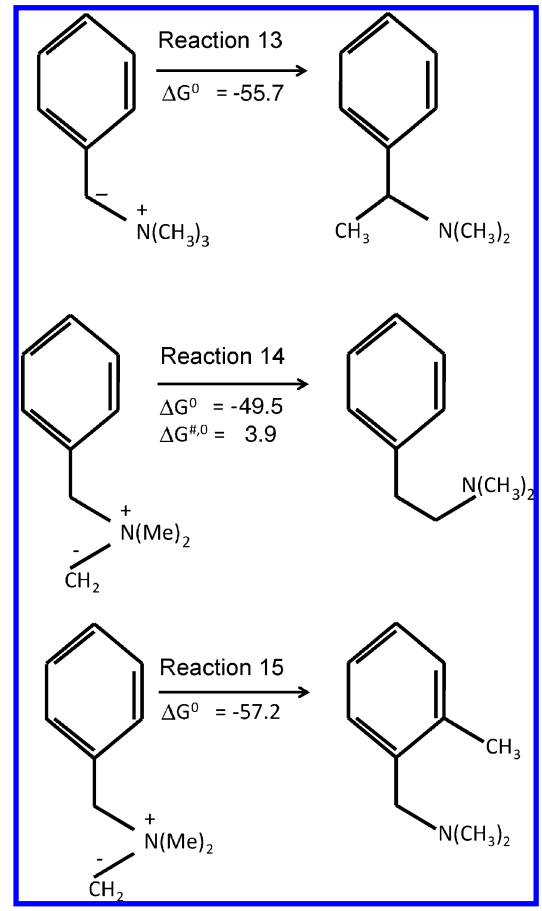

Figure 7. Rearrangements of ylide to give thermodynamically stable products.

Another reason to take the ylide path into account was the possibility of side reactions that may pass through the reactive ylide intermediate. In the case of benzyl-TMA the rearrangements shown in Figure 7 have been identified as possible reactions.[4,17] Reactions 13 and 14 in Figure 7 are Stevens rearrangement reactions,[15,17−20,34,35] whereas reaction 15 in Figure 7 is the Sommelet−Hauser rearrangement.[15,17,20] Our DFT calculations show that these reactions are highly favored from a thermodynamic point of view, with large negative changes in free energy. We were able to calculate the barrier for one of the Steven rearrangement steps (reaction 14, Figure 7). The activation barrier for this rearrangement is very low ($\Delta E^{\ddagger} = 6.3$ kcal/mol, $\Delta G^{\ddagger,0} = 3.9$ kcal/mol). The total $\Delta G^{\ddagger,0}$ for the degradation through a ylide pathway can be estimated by adding the ΔG^0 from reaction 6 in Table 1. Thus the total barrier for degradation through reactions 6 and 14 is 17.1 kcal/mol, which is slightly lower than the 18.6 kcal/mol for the S_N2 pathway.

We were not able to find low-lying transition states for reactions 13 and 15 in Figure 7. The estimated barriers for these two reactions were too high (>40 kcal/mol). However, there

may be lower energy pathways that correspond to different spin states (for example, singlet, triplet, or a broken symmetry singlet) that play a role for these reactions and our restricted B3LYP theory might have missed some other lower energy pathways for reactions 13 and 15 (Figure 7). Past work on the Stevens rearrangement suggests that this reaction may proceed through an ion-pair, concerted-shift, or radical-pair pathway.[34,35] The transition state identified for reaction 14 in Figure 7 corresponds to the one suggested by Thomson and Stevens.[34] This transition state has a very high dipole moment of 11 D, whereas the reactant ylide has a dipole moment of 7 D. This implies that the transition state is further stabilized by the polar medium, lowering the overall barrier. At this point we do not rule out the radical-pair pathway, and there is clearly a need for further studies on these rearrangements. However, we have shown that there exists at least one ylide pathway (reaction 6, followed by reaction 14 in Figure 7) by which benzyl-TMA might be expected to degrade at a rate comparable to that of S_N2 and contribute in a meaningful way to the loss of ammonium groups in a membrane.

Conclusions

We have extended upon our previous work in which we examined the S_N2 and ylide pathways of degradation of tetraalkylammonium ions. The current results show that it is important to consider the immediate neighborhood of the reaction center in more detail while studying OH^- reactions. Our explicit model in which the solvation shell was modeled in detail gives activation barriers that more closely reflect experimental observation. A detailed study of benzyl-TMA degradation shows that the energy changes and activation barriers are very close to that of TMA degradation. However, we show that further ylide rearrangements can occur from benzyl-TMA through Stevens and Sommelet−Hauser rearrangements. Thus a combination of S_N2 and ylide formation followed by Stevens and Sommelet−Hauser rearrangements are expected to lead to the degradation of cationic fuel cell membranes. Hofmann elimination is also expected to contribute to degradation in the case of cations with β hydrogen.

Acknowledgment. This project was funded by the U.S. Department of Energy, Office of Basic Energy Sciences, Division of Materials Sciences and Engineering.

Supporting Information Available: Cartesian coordinates of transition states in *xyz* format and the reaction path configurations for H−D exchange. This material is available free of charge via the Internet at http://pubs.acs.org.

References and Notes

(1) Hatch, M. J.; Lloyd, W. D. *J. Appl. Polym. Sci.* **1964**, *8*, 1659.
(2) Baumann, E. W. *J. Chem. Eng. Data* **1960**, *5*, 376.
(3) Tanaka, J.; Dunning, J. E.; Carter, J. C. *J. Org. Chem.* **1966**, *31*, 3431.
(4) Archer, D. A. *J. Chem. Soc. C* **1971**, 1329.
(5) Musker, W. K. *J. Am. Chem. Soc.* **1964**, *86*, 960.
(6) Chempath, S.; Einsla, B. R.; Pratt, L. R.; Macomber, C. S.; Boncella, J. M.; Rau, J. A.; Pivovar, B. S. *J. Phys. Chem. C* **2008**, *112*, 3179.
(7) Varcoe, J. R.; Slade, R. C. T. *Fuel Cells* **2005**, *5*, 187.
(8) Asazawa, K.; Yamada, K.; Tanaka, H.; Oka, A.; Taniguchi, M.; Kobayashi, T. *Angew. Chem., Int. Ed.* **2007**, *46*, 8024.
(9) Lu, S.; Pan, J.; Huang, A.; Zhuang, L.; Lu, J. *Proc. Natl. Acad. Sci. U.S.A.* **2008**, *105*, 20611.
(10) Spendelow, J. S.; Wieckowski, A. *Phys. Chem. Chem. Phys.* **2007**, *9*, 2654.
(11) Einsla, B. R.; Chempath, S.; Pratt, L.; Boncella, J.; Rau, J.; Macomber, C.; Pivovar, B. *ECS Trans.* **2007**, *11*, 1173.
(12) Iojoiu, C.; Chabert, F.; Maréchal, M.; Kissi, N. E.; Guindet, J.; Sanchez, J. Y. *J. Power Sources* **2006**, *153*, 198.
(13) Joseph, J.-G. *Polym. Adv. Technol.* **2007**, *18*, 785.
(14) Tomoi, M.; Yamaguchi, K.; Ando, R.; Kantake, Y.; Aosaki, Y.; Kubota, H. *J. Appl. Polym. Sci.* **1997**, *64*, 1161.
(15) Kantor, S. W.; Hauser, C. R. *J. Am. Chem. Soc.* **1951**, *73*, 4122.
(16) Thomson, T.; Stevens, T. S. *J. Chem. Soc.* **1931**, 55.
(17) Maeda, Y.; Sato, Y. *J. Chem. Soc., Perkin Trans.* **1997**, *1*, 1491.
(18) Heard, G. L.; Yates, B. F. *Aust. J. Chem.* **1994**, *47*, 1685.
(19) Heard, G. L.; Yates, B. F. *J. Comput. Chem.* **1996**, *17*, 1444.
(20) Heard, G. L.; Yates, B. F. *J. Org. Chem.* **1996**, *61*, 7276.
(21) Frisch, M. J.; Trucks, G. W.; Schlegel, H. B.; Scuseria, G. E.; Robb, M. A.; Cheeseman, J. R.; Montgomery, J. A., Jr.; Vreven, T.; Kudin, K. N.; Burant, J. C.; Millam, J. M.; Iyengar, S. S.; Tomasi, J.; Barone, V.; Mennucci, B.; Cossi, M.; Scalmani, G.; Rega, N.; Petersson, G. A.; Nakatsuji, H.; Hada, M.; Ehara, M.; Toyota, K.; Fukuda, R.; Hasegawa, J.; Ishida, M.; Nakajima, T.; Honda, Y.; Kitao, O.; Nakai, H.; Klene, M.; Li, X.; Knox, J. E.; Hratchian, H. P.; Cross, J. B.; Bakken, V.; Adamo, C.; Jaramillo, J.; Gomperts, R.; Stratmann, R. E.; Yazyev, O.; Austin, A. J.; Cammi, R.; Pomelli, C.; Ochterski, J. W.; Ayala, P. Y.; Morokuma, K.; Voth, G. A.; Salvador, P.; Dannenberg, J. J.; Zakrzewski, V. G.; Dapprich, S.; Daniels, A. D.; Strain, M. C.; Farkas, O.; Malick, D. K.; Rabuck, A. D.; Raghavachari, K.; Foresman, J. B.; Ortiz, J. V.; Cui, Q.; Baboul, A. G.; Clifford, S.; Cioslowski, J.; Stefanov, B. B.; Liu, G.; Liashenko, A.; Piskorz, P.; Komaromi, I.; Martin, R. L.; Fox, D. J.; Keith, T.; Al-Laham, M. A.; Peng, C. Y.; Nanayakkara, A.; Challacombe, M.; Gill, P. M. W.; Johnson, B.; Chen, W.; Wong, M. W.; Gonzalez, C.; Pople, J. A. *Gaussian 03*, Revision C.02; Gaussian, Inc., Wallingford, CT, 2004.
(22) Peters, B.; Heyden, A.; Bell, A. T.; Chakraborty, A. *J. Chem. Phys.* **2004**, *120*, 7877.
(23) Macomber, C.; Boncella, J.; Pivovar, B.; Rau, J. *J. Therm. Anal. Calorim.* **2008**, *93*, 225.
(24) Musker, W. A. *J. Chem. Educ.* **1968**, 200.
(25) Robertson, W. H.; Diken, E. G.; Price, E. A.; Shin, J. W.; Johnson, M. A. *Science* **2003**, *299*, 1367.
(26) Imberti, S.; Botti, A.; Bruni, F.; Cappa, G.; Ricci, M. A.; Soper, A. K. *J. Chem. Phys.* **2005**, *122*, 194509.
(27) Smiechowski, M.; Stangret, J. *J. Phys. Chem. A* **2007**, *111*, 2889.
(28) Cappa, C. D.; Smith, J. D.; Messer, B. M.; Cohen, R. C.; Saykally, R. J. *J. Phys. Chem. A* **2007**, *111*, 4776.
(29) Megyes, T.; Balint, S.; Grósz, T.; Radnai, T.; Bako, I.; Sipos, P. *J. Chem. Phys.* **2007**, *128*, 044501.
(30) Tuckerman, M. E.; Marx, D.; Parrinello, M. *Nature* **2002**, *417*, 925.
(31) Tuckerman, M. E.; Chandra, A.; Marx, D. *Acc. Chem. Res.* **2006**, *39*, 151.
(32) Aziz1, E. F.; Ottosson, N.; Faubel, M.; Hertel, I. V.; Winter, B. *Nature* **2008**, *455*, 89.
(33) Asthagiri, D.; Pratt, L. R.; Kress, J. D.; Gomez, M. A. *Proc. Natl. Acad. Sci. U.S.A.* **2004**, *101*, 7229.
(34) Thomson, T.; Stevens, T. S. *J. Chem. Soc.* **1932**, 55.
(35) Vanecko, J. A.; Wan, H.; West, F. G. *Tetrahedron* **2006**, *62*, 1043.

JP9122198